Determination of Radiation Dose Level Exposed to Thyroid in C-Arm Scopy

Muhammed Selim ÖZLEN[1*], Ayşe Beyza CUMA[2], Selma Dilara YAZICI[3], Nami YEĞİN[4], Özge DEMİR[5], S. Hilmi AKSOY[6], Eylem KEKEÇ[7], Tülin ZENGİN[8], Osman GÜNAY[9]

[1]Yildiz Technical University, Electrics and Electronics Faculty, Biomedical Engineering Dep. Istanbul-Turkiye
* Corresponding Author Email: selim.ozlen@std.yildiz.edu.tr – **ORCID:** 0009-0002-1016-6277

[2]Yildiz Technical University, Electrics and Electronics Faculty, Biomedical Engineering Dep. Istanbul-Turkiye
Email: beyza.cuma@std.yildiz.edu.tr – **ORCID:** 0009-0007-6709-5437

[3] Yildiz Technical Univ., Electrics and Electronics Faculty, Biomedical Engineering Dep., Istanbul-Turkiye
Email: dilara.yazici@std.yildiz.edu.tr – **ORCID:** 0009-0006-1456-604X

[4] Dep. of Nuclear Medicine, Cerrahpasa Faculty of Medicine, Istanbul University-Cerrahpasa, Istanbul, Turkey
Email: namiyeyin@gmail.com - ORCID: 0000-0003-0262-4020

[5] Istanbul University – Cerrahpasa, Faculty of Engineering, Department of Chemical Engineering, Department of Unit Operations and Thermodynamics, 34315, Istanbul – Turkey.
Email: ozge.demir@iuc.edu.tr - ORCID: 0000-0002-0342-5915

[6]Department of Radiology, Hisar Intercontinental Hospital, Istanbul, Turkey, Istanbul – Turkey.
Email: hilmi.aksoy@hisarhospital.com - ORCID: 0000-0002-2356-0268

[7]Nuclear Energy Research Institute, Secondary Standard Dosimetry Laboratory, Istanbul, Turkiye
Email: eylemkekec2@gmail.com - ORCID 0009-0007-7477-4665

[8]Nuclear Energy Research Institute, Secondary Standard Dosimetry Laboratory, Istanbul, Turkiye
Email: tulin.zengin@tenmak.gov.tr - ORCID 0009-0002-6781-647X

[9]Yildiz Technical University, Electrics and Electronics Faculty, Biomedical Engineering Dep. Istanbul-Turkiye
Email: ogunay@yildiz.edu.tr - 0000-0003-0760-554X

Abstract:

This study aims to evaluate the radiation dose impacting thyroid tissue during C-arm fluoroscopy using the Alderson Rando phantom and thermoluminescent dosimeters (TLD-100). Given the sensitivity of the thyroid, understanding the dose is crucial for patient safety.The Alderson Rando phantom, representing a human equivalent, was employed for radiation exposure assessment. TLD-100 dosimeters were strategically placed in the thyroid region of the phantom's 9th section. Measurements were taken at 0.5, 1, 2, 4, and 8-minute intervals. The study was conducted at Istanbul University-Cerrahpasa, with the Alderson Rando phantom sourced from the Department of Radiation Oncology. Evaluation of research findings occurred at the Cekmece Nuclear Research Center.The study revealed the average radiation dose impacting thyroid internal tissue as 0.760 mSv (0.5 minutes), 1.319 mSv (1 minute), 2.7345 mSv (2 minutes), 5.633 mSv (4 minutes), and 11.5595 mSv (8 minutes).

The average radiation dose affecting thyroid skin tissue was found to be 1.587 mSv (0.5 minutes), 2.3905 mSv (1 minute), 5.0075 mSv (2 minutes), 9.8115 mSv (4 minutes), and 18.8635 mSv (8 minutes).Minimizing radiation dose is crucial to reduce potential harm to patients. However, the absence of established reference values in the literature emphasizes the need for determining this dose, as no standardized benchmark currently exists. Annual radiation dose limits for various body parts exist, but establishing specific values for thyroid tissue during C-arm fluoroscopy is essential for enhancing patient safety in radiological procedures.

1. Introduction

X-rays, electromagnetic waves capable of ionizing atoms, play a pivotal role in medical imaging techniques such as computed tomography (CT), conventional X-rays, mammography, and fluoroscopy (C-arm scopy). The penetration of patient tissue by X-rays is imperative for effective imaging.

Radiation, inherent in these imaging processes, poses potential harm to the human body, leading to issues such as cancer, radiation burns, a shortened lifespan, and hereditary disorders [1]. Medical applications constitute a primary source of artificial radiation exposure, with a global average of 0.3 mSv per person annually [2]. Sensitivity to radiation varies among different body parts, with active tissues exhibiting higher susceptibility [3,4]. Notably, research indicates an elevated risk of thyroid cancer in the presence of radiation or X-rays [5-7]. The thyroid gland, being an active tissue, is particularly sensitive to radiation. Consequently, understanding the extent of radiation exposure is crucial for patient health and treatment.According to the International Commission on Radiation Protection (ICRP) guidelines, maximum ionizing radiation doses deemed safe for humans are specified as follows: 50 mSv and 1 mSv for the whole body of radiation workers and other individuals; 50 mSv and 15 mSv for the pupils of the eyes; 500 mSv and 50 mSv for the hands, feet, and skin of both radiation workers and other persons [8]. The defined harm encompasses genetic effects or the onset of diseases. To minimize the harmful effects of radiation, it is essential to first determine the levels of radiation exposure. Therefore, extensive research has been conducted using various methods to determine both natural radiation levels and artificial radiation levels, such as X-rays [9-18].This study focuses on simulating and determining the radiation exposure to the thyroid gland of patients undergoing C-arm imaging using a phantom. Quantifying patient radiation exposure during fluoroscopy employed the Alderson Rando phantom, utilizing ten Thermoluminescent Dosimeters (TLDs). The visual representation of the cranial region of the phantom was simulated for varying durations: 0.5, 1, 2, 4, and 8 minutes, with corresponding radiation measurements obtained by reading the TLDs.

2. Materials and Methods

In this study, the Alderson Rando phantom **(Fig 1)** (The Alderson Radiation Therapy Phantom, ART), designed to mimic an adult human closely, will be utilized. The phantom is enveloped in acrylic with the same density as human tissue and comprises human bones [19]. Designed to yield realistic outcomes in studies on tissues and organs, the Alderson Rando Phantom will be procured from Istanbul University-Cerrahpaşa, Cerrahpaşa Faculty of Medicine, Radiation

Oncology, and adheres to ICRU-44 standards [20]. This female representation is 155 cm long and weighs 50 kg, with a material density of 0.985 g/cm³ [21]. The phantom consists of 32 sections, each 2.5 cm thick, with embedded pins for affixing TLD dosimeters for measuring absorbed doses [20].

Figure 1: Alderson Rando Female Phantom (ART) [22].

The study employs TLDs, a widely used method for calculating radiation doses [19, 23, 24]. 12 TLD-100 dosimeters **(Fig 2)** with dimensions of 0.89 mm thickness, 3.2 mm width, and 3.2 mm length, containing LiF, Mg, and Ti [23], were used. For calibration, all TLD-100s underwent annealing in an oven at 400°C for 1 hour, followed by 100°C for 2 hours. The relative standard deviation of the TLDs was maintained below 3% [23]. The TLD-100 chips included in the research were read after their calibration and imaging with C-arm scopy in the secondary standard dosimetry (SSDL) laboratory at TENMAK Çekmece Nuclear Research Center. The readings of radiation dose measurements were carried out using the Harshaw 4500 model TLD reader connected to a computer, utilizing the WinREMS software, also located in the same laboratory [21]. Heat-generating nitrogen gas is used to heat the TLD reading system. The element correction coefficients (ECCs) of the TLD chips and the reader calibration factor (RCF) of the TLD reader were acquired by measurements made at SSDL using a standard Cs-137 gamma source, in accordance with the WinDEMS software user manual. Cs-137 source and Yxlon International MGC 41 model X-ray system were used for the calibration of the reader [21]. Reference standard dosimeters were utilized for measuring the dose rate of radiation. C-arm fluoroscopy imaging **(Fig 3)** was carried out in automatic settings in the Radiology unit of Istanbul University-Cerrahpaşa, Cerrahpaşa Faculty of Medicine. Imaging of the phantom was performed with the C-arm scopy at Cerrahpaşa Medical Faculty. After calibration, ten TLD-100s were affixed to the thyroid area needles on the phantom. As per the Alderson Rando female phantom, the thyroid is located in the 9th section. Two localizations in the 9th section were chosen for the measurement process, with 2 TLD chips placed vertically and separately in each localization. Images were captured in this region under C-arm fluoroscopy for 0.5, 1, 2, 4, and 8 minutes, respectively. For each period, previous TLDs were replaced with 2 new TLD chips. A total of 5 separate shots were taken for the thyroid region using 10 TLD-100 chips. 2 TLD-100 chips were dedicated to determining the background radiation levels and the radiation exposure to the operator, remaining in the background throughout the irradiation processes.

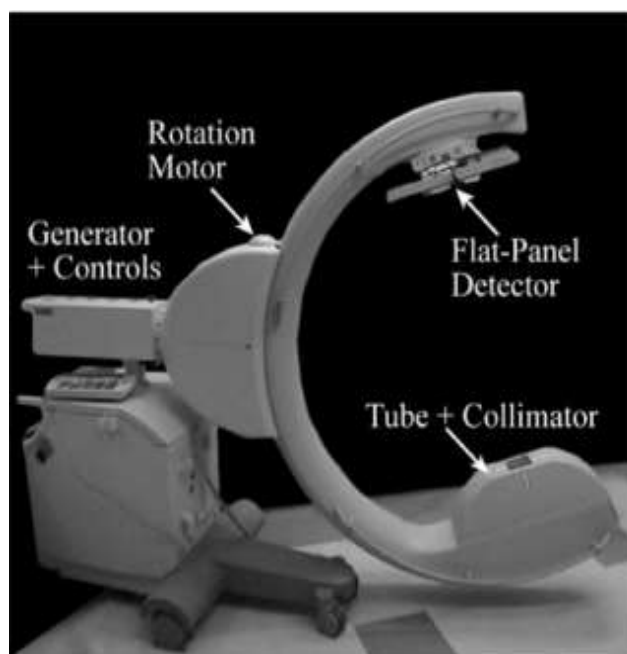***Figure 2:*** *Thermoluminescent Dosimeters*

Figure 3: *C-arm Scopy [25]*

Referencing the dose affecting the environment is crucial for calculating the radiation dose to which the thyroid area is exposed. After the completion of imaging, radiation exposure values for TLDs were measured at the Çekmece Nuclear Research Center (TENMAK). Each average radiation value obtained from five different time intervals was independently calculated. A graph of the experiment was created using the obtained data and time correlation. The duration of fluoroscopy reaching the maximum radiation dose was determined through mathematical calculations. Standard deviation and mean calculations were performed using simple statistical methods. Thus, the radiation dose to the thyroid gland during C-arm fluoroscopy imaging was calculated.

3. Results and Discussions
The experiments have determined minimum and maximum values for both thyroid skin tissue and thyroid internal tissue. According to the results of the conducted experiments, variable

outcomes were obtained concerning time. These results indicated a proportional increase in the radiation dose affecting the thyroid as the exposure time increased. The values indicating a direct proportionality between time and radiation dose have been observed. Additionally, it was observed that the radiation dose affecting the inner part of the thyroid tissue is lower than the outer part. The average radiation dose affecting the thyroid skin is determined to be: **(Table 1)** 1.587 mSv for half a minute, 2.390 mSv for 1 minute, 5.007 mSv for 2 minutes, 9.811 mSv for 4 minutes, and 18.863 mSv for 8 minutes. The minimum and maximum values affecting the thyroid skin, respectively were found to be: 1.324 and 1.850 mSv for half a minute, 2.214 and 2.567 mSv for 1 minute, 4.891 and 5.124 mSv for 2 minutes, 9.267 and 10.356 mSv for 4 minutes, 16.382 and 21.345 mSv for 8 minutes. As seen in **Figure 4**, the R^2 value for the thyroid skin is 0.9994. In this study, the average radiation dose affecting the intrathyroidal area is determined to be: **(Table 2)** 0.760 mSv for half a minute, 1.319 mSv for 1 minute, 2.734 mSv for 2 minutes, 5.633 mSv for 4 minutes, and 11.559 mSv for 8 minutes. The minimum and maximum radiation doses affecting the intrathyroidal area were found to be: 0.654 and 0.867 mSv for half a minute, 1.186 and 1.452 mSv for 1 minute, 2.445 and 3.024 mSv for 2 minutes, 5.128 and 6.138 mSv for 4 minutes, 9.268 and 13.850 mSv for 8 minutes. As seen in **Figure 5**, the R^2 value for the intrathyroidal region is 0.9996.

***Table 1:** Values of the radiation dose that affects the thyroid skin.*

Time (minute)	Thyroid Skin Average Value (mSv)	Thyroid Skin Minimum Value (mSv)	Thyroid Skin Maximum Value (mSv)
0.5	1.587	1.324	1.850
1	2.390	2.214	2.567
2	5.007	4.891	5.124
4	9.811	9.267	10.356
8	18.863	16.382	21.345

***Table 2:** Values of the radiation dose that affects the intrathyroidal area.*

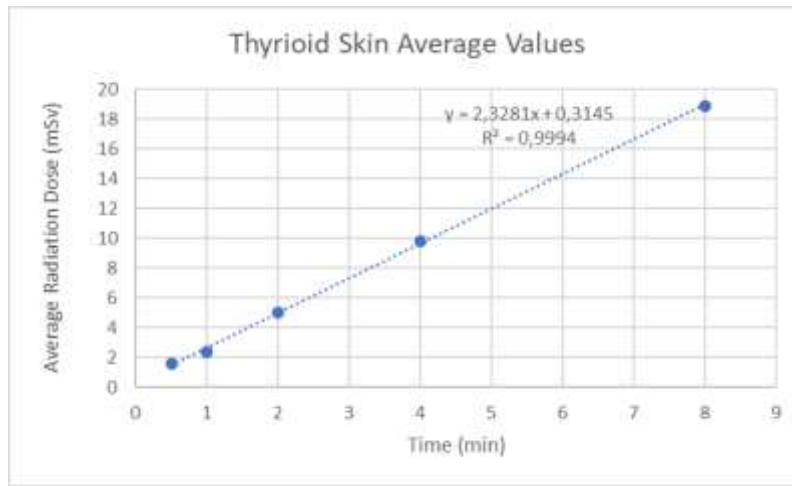| Time (minute)	Intrathyroidal Average Value (mSv)	Intrathyroidal Minimum Value (mSv)	Intrathyroidal Maximum Value (mSv)
0.5	0.760	0.654	0.867
1	1.319	1.186	1.452
2	2.734	2.445	3.024
4	5.633	5.128	6.138
8	11.559	9.268	13.85

Figure 4: *The representation, along with the equation, for radiation dose absorbed by the thyroid on the skin surface.*
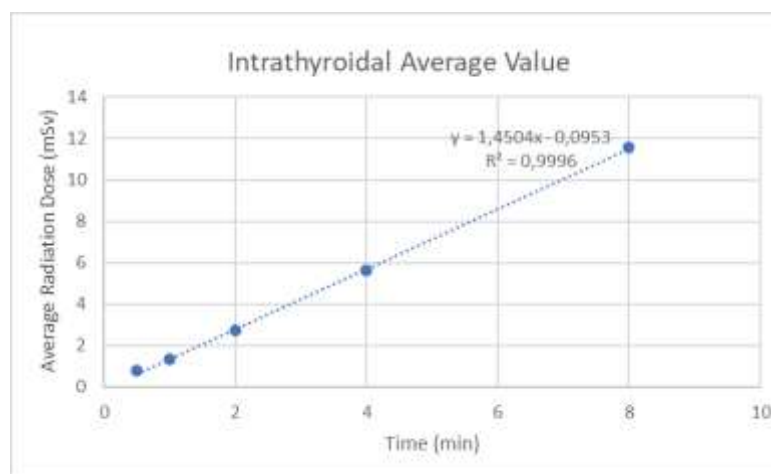

Figure 5: *The representation, along with the equation, of the amount of radiation dose absorbed on the inner surface of the thyroid.*

The line graphs were generated based on the averages of the obtained values. The equations for these graphs were determined, and the R^2 values were calculated. An R^2 value approaching 1 indicates a strong correlation in the equation. According to these calculations, it has been observed that the ratio of the influencing radiation dose is directly proportional to time. This suggests that, as time increases, the radiation dose exhibits a direct relationship. The closer the R^2 value is to 1, the more indicative it is of the accuracy of the correlation in the equation.

The study's results revealed varying average radiation doses affecting the thyroid gland during C-arm fluoroscopy imaging. For the inner tissue of the thyroid, the measured doses increased progressively with longer exposure times: 0.760 mSv for 0.5 minutes, 1.319 mSv for 1 minute, 2.7345 mSv for 2 minutes, 5.633 mSv for 4 minutes, and 11.5595 mSv for 8 minutes. Similarly, the average radiation doses affecting the thyroid skin tissue exhibited an ascending trend: 1.587 mSv for 0.5 minutes, 2.3905 mSv for 1 minute, 5.0075 mSv for 2 minutes, 9.8115 mSv for 4 minutes, and 18.8635 mSv for 8 minutes.

These findings provide crucial insights into the quantification of radiation exposure during C-arm fluoroscopy, emphasizing the importance of optimizing safety measures in medical imaging to mitigate potential health risks for both patients and healthcare professionals involved in such procedures.

Radiation refers to the process of energy propagation from atoms to the environment. This energy arises from the imbalance of neutrons and protons in the atomic nucleus [26,27]. Radiation can propagate as electromagnetic waves or particles and is divided into two main classes: ionizing and non-ionizing radiation. Ionizing radiation includes radiation with energy levels capable of removing an electron from an atom [27]. X-rays and gamma rays are two types of electromagnetic waves with the ability to ionize atoms and are commonly used in medical imaging techniques such as CT, X-rays, mammography, and fluoroscopy [26].

C-arm fluoroscopy is a significant medical imaging technique that provides real-time imaging using X-rays in a C-shaped configuration. This technology is utilized in various medical fields such as orthopedics, cardiology, and vascular surgery. The capability of high-quality simultaneous imaging allows surgeons to see the internal structures of patients in detail, facilitating more effective and safe surgical interventions, especially by reducing the duration of the surgery.

Due to its wide-angle imaging capacity facilitated by the C-shaped arm structure, C-arm fluoroscopy enables surgeons to visualize the patient's internal structures in a detailed and clear manner during surgery. As a subfield in radiology, C-arm fluoroscopy is based on obtaining images by injecting radiation into the body. This technique is a crucial tool in medicine, offering real-time imaging during surgical interventions and being applicable in various medical disciplines.

However, it is known that radiation has harmful effects on the human body, including cancer, radiation burns, shortened lifespan, and genetic disorders [1]. Radiation can ionize or excite atoms and molecules in tissues. The resulting radical atoms and molecules can harm the organism's structure, cause damage to chromosomes, and be transmitted to subsequent generations through gene transfer, a phenomenon known as mutation (genetic disorder).

Artificial radiation used for medical purposes is the most common source of radiation exposure for humans, with a global average of 0.3 mSv per person per year [2]. Additionally, each part of the body has different sensitivities to radiation, with more active tissues generally being more sensitive [3,4]. Research indicates that the presence of radiation or X-rays may increase the risk of thyroid cancer [5-7]. The thyroid gland, which regulates the body's basic metabolism by producing hormones, is particularly sensitive to radiation.

In this context, it is crucial to know the amount of radiation exposure for patients to minimize harm to their health during the treatment process. Various methods have been developed to protect against the harmful effects of radiation, aiming to protect both patients and imaging technicians. These measures can be applied under three main categories: distance from the radiation source, time spent in the radiation environment, and the received dose [28]. Among the precautions are technicians having a separate office outside the imaging room, using screening rooms, applying radiation in optimal doses, and using protective equipment (e.g., lead aprons, goggles, gloves, and thyroid protectors).

Maximum ionizing radiation doses specified by the ICRP are crucial for safeguarding the health of individuals exposed to radiation. These doses indicate the maximum amount of radiation that a radiation worker and a general individual can receive annually for different body regions [8]. These rules aim to prevent any radiation-induced bodily illness or genetic effects.

The maximum ionizing radiation dose limits deemed non-harmful for humans, as stipulated by the ICRP, are as follows: **(Table 3)** In the context of annual radiation exposure limits, a radiation worker and an ordinary individual can receive a maximum dose of 50 mSv and 5 mSv,

respectively, for the entire body. For specific areas such as hands, feet, and the entire skin, the permissible annual radiation dose is 500 mSv for a radiation worker and 50 mSv for an ordinary individual. Additionally, concerning the annual dose limit for the pupil of the eye, it is 150 mSv for a radiation worker and 15 mSv for an ordinary individual. [8]. The term 'harm' mentioned here refers to any potential adverse health effects or genetic impacts.

Table 3: Annual maximum ionizing radiation dose limits deemed non-harmful for humans as specified by the ICRP.

	Radiation Workers (mSv)	General Public Individuals (mSv)
Whole Body	50	5
Hands, Feet, and Skin	500	50
Lens of the Eye	150	15

This study aimed to determine the amount of radiation patients are exposed to during C-arm imaging and inform technicians using the device about maximum radiation values. In pursuit of this goal, radiation exposure to thyroid glands during the automatic mode imaging of the cranial region of patients was measured for 0.5, 1, 2, 4, and 8 minutes.

This study draws inspiration from previous research on the exposure of hospital personnel to radiation during orthopedic surgeries [28]. In that study, radiation exposure levels for personnel were measured using OSL dosimeters placed at various distances during surgery. Based on the average monthly radiation levels detected by the dosimeters, the level of personnel exposure to radiation was determined.

Another study examined the amount of radiation patients are exposed to during CT scans [29]. Using the Alderson Rando phantom, this study evaluated the radiation exposure of patients' thyroid, lens, and oral mucosa regions during CT scans. The results of this study highlight exposure levels in different areas, providing valuable information to understand potential health risks associated with radiation.

This current study, taking inspiration from these two significant studies in the literature, aims to determine the amount of radiation patients are exposed to during fluoroscopy imaging. Within the scope of the study, fluoroscopy imaging was performed for 0.5, 1, 2, 4, and 8 minutes in automatic mode in the simulated cranial region using Alderson Rando phantom, and radiation values were measured using 12 TLD dosimeters.

As a result of the study, the radiation doses to which the thyroid gland is exposed were determined. In addition, as can be seen from the graphs (**Figures 5** and **6**), the R^2 value is very close to one. This is proof that the dependent variable in this study is changed only by the dependent variable (In this study, the dependent and independent variables are dose amount and time, respectively). In other words, according to the study's results, the duration of use of the C-arm scopy should be optimized so that the dose amount received by the patients can be adjusted according to the values of ICRP in order not to cause extra harm to the patient.

The unique contribution of this study lies in calculating the amount of radiation patients are exposed to during fluoroscopy imaging. The fact that patients are exposed to radiation is well-established, and the serious effects of this radiation on human health have been emphasized.

However, there needs to be sufficient research on this specific topic in the literature. Therefore, this study should be regarded as a crucial step in identifying these critical dose levels for the safety of patients.

4. Conclusion

In summary, this study found that the thyroid was exposed to considerable radiation during C-arm scoping. The conclusion underscores the critical importance of monitoring radiation dose exposure, particularly in sensitive anatomical regions such as the thyroid, during these procedures. Determining the level of radiation dose exposure to the thyroid gland is a vital step in enhancing the safety of such medical imaging procedures. However, since no reference values are established in the literature and there is currently no standardized benchmark, it is concluded that there is a need to determine this dose and increase patient safety with optimizations made in light of this data. Suggestions for future research directions, such as conducting similar studies on different patient groups or assessing the effects of various C-arm fluoroscopy procedures on the thyroid, could further enhance the understanding of the study's findings and provide additional insights. Additionally, research focusing on strategies to reduce radiation dose exposure or more effective protection methods is crucial. For this study to provide more clinical data for the literature, more clinical studies are needed on phantoms of varying sizes with different models of devices with different durations.

References

[1]Tuncel, E. (2008). Klinik Radyoloji. Nobel & Güneş Tıp Kitabevleri.

[2]Bora, H. (2001). Radyasyon güvenliği. Ankara Üniversitesi Dikimevi Sağlık Hizmetleri Meslek. 2(1), 91-98. https://doi.org/10.1501/ashd_0000000023

[3]Şeker, S. S., & Çerezci, O. (1997). Çevremizdeki radyasyon ve korunma yöntemleri (1. bs.). Boğaziçi Üniversitesi Yayınları. İstanbul, Turkey: Boğaziçi Üniversitesi.

[4]Şeker, S., & Çerezci, O. (2000). Radyasyon Kuşatması. Boğaziçi Üniversitesi Yayınevi-matbaası, İstanbul.

[5]Fidancı, İ., Tekin, O., Demirel, A. H., Arslan, İ., Dilber, S., Eren, Ş. Ü., & Gümüş, E. (2014). Radyasyon üreten Cihazların Kullanımı Ile Tiroid Kanseri Arası ilişkinin Değerlendirilmesi. Ankara Medical Journal, 14(3). https://doi.org/10.17098/amj.37721

[6]de González, A. B., & Darby, S. (2004). Risk of cancer from Diagnostic X-rays: Estimates for the UK and 14 other countries. The Lancet, 363(9406), 345–351. https://doi.org/10.1016/s0140-6736(04)15433-0

[7] Hall, E. J., & Brenner, D. J. (2008). Cancer risks from Diagnostic Radiology. The British Journal of Radiology, 81(965), 362–378. https://doi.org/10.1259/bjr/01948454

[8] Karataşlı, M., & Tahsin, Ö. Z. E. R. (2018). İş güvenliğinde dozimetreler. İstanbul Aydın Üniversitesi Dergisi, 10(1), 15-31.

[9] Akkurt, I., & Boodaghi Malidarre, R. (2021). Gamma photon-neutron attenuation parameters of marble concrete by MCNPX code. Radiation Effects and Defects in Solids, 176(9-10), 906-918.

[10] Akkurt, I., & Tekin, H. O. (2020). Radiological parameters for bismuth oxide glasses using phy-X/PSD software. Emerging Materials Research, 9–3, 1020–1027. https://doi.org/10.1680/jemmr.20.00209

[11] Boodaghi Malidarre, R., Akkurt, İ., Gunoglu, K., Akyıldırım, H. (2021). Fast Neutrons Shielding Properties for HAP-Fe2O3 Composite Materials. International Journal of Computational and Experimental Science and Engineering, 7(3), 143-145. https://doi.org/10.22399/ijcesen.1012039

[12] Celen, Y. Y., Oncul, S., Narin, B., & Gunay, O. (2023). Measuring radon concentration and investigation of it's effects on lung cancer. Journal of Radiation Research and Applied Sciences, 16(4), 100716.

[13] Günay, O., Gündoğdu, Ö., Demir, M., Abuqbeitah, M., Yaşar, D., Aközcan, S., ... & Yarar, O. (2019). Determination of the radiation dose level in different slice computerized tomography. International Journal of Computational and Experimental Science and Engineering, 5(3), 119-123.

[14] Günay, O., Sarihan, M., Abamor, E., & Yarar, O. (2019). Environmental radiation doses from patients undergoing Tc-99m DMSA cortical renal scintigraphy. International Journal of Computational and Experimental Science and Engineering, 5(2), 86-93

[15] Günay, O., Özden, S., & Pehlivanoğlu, S. A. (2023). Assessing the Topsoil Contamination of Cesium-137 Environmental Fallout in Konya, Turkey: Spatial Distribution and Analysis. Water, Air, & Soil Pollution, 234(12), 763

[16] Özden, S., Aközcan, S., & Günay, O. (2023). 137Cs in Soils from İstanbul (Turkey) Sampled 35 Years After Chernobyl. Environmental Forensics, 1-7.

[17] Sen Baykal, D., Tekin, H., & Çakırlı Mutlu, R. (2021). An investigation on radiation shielding properties of borosilicate glass systems. International Journal of Computational and Experimental Science and Engineering, 7(2), 99–108. https://doi.org/10.22399/ijcesen.960151

[18] Tekin, H. O., Cavli, B., Altunsoy, E. E., Manici, T., Ozturk, C., & Karakas, H. M. (2018). An investigation on radiation protection and shielding properties of 16 slice computed tomography (CT) facilities. International Journal of Computational and Experimental Science and Engineering, 4–2, 37–40. https://doi.org/10.22399/ijcesen.408231

[19] Lee, K., Lee, K. M., Park, M. S., Lee, B., Kwon, D. G., & Chung, C. Y. (2012). Measurements of surgeons' exposure to ionizing radiation dose during intraoperative use of C-arm fluoroscopy. Spine, 37(14), 1240-1244.

[20] Radiation Products Design, Inc. https://www.rpdinc.com/

[21] Günay, O., & Demir, M. (2019). Bilgisayarlı Tomografi Çekimlerinde Hastanın Yakın Çevresinde Radyasyon Dozu Ölçümleri. Süleyman Demirel Üniversitesi Fen Bilimleri Enstitüsü Dergisi, 23(3), 792-796.

[22] Acquah, G.F., Kyeremeh, P.O., Doudoo, C.O., Ahiagbenyo, P., Edusa, C., & Beecham, K. (2017). Breast Dosimetry: A Phantom study between tangential wedge fields and multiple open field-in-field 3D conformal forward planning. International Journal of Scientific Research in Science and Technology, 3, 196-200.

[23] Başaran, H., Gül, O. V., & Gökçen, İ. N. A. N. (2022). Farklı Radyoterapi Teknikleri İle Meme Işınlamalarında Alan Dışı Dozların TLD İle Dozimetrik Olarak İncelenmesi. Akdeniz Tıp Dergisi, 8(3), 270-275.

[24] Şahmaran, T., & Bayburt, M. (2020). Pozitron Emisyon Tomografi–Bilgisayar Tomografi (PET-BT) uygulamalarında hastanın aldığı radyasyon dozunun belirlenmesi. Kafkas Üniversitesi Fen Bilimleri Enstitüsü Dergisi, 13(1), 58-63.

[25] Siewerdsen, J. H., Moseley, D. J., Burch, S., Bisland, S. K., Bogaards, A., Wilson, B. C., & Jaffray, D. A. (2005). Volume CT with a flat- panel detector on a mobile, isocentric C- arm: pre- clinical investigation in guidance of minimally invasive surgery. Medical physics, 32(1), 241-254.

[26] Gökharman, D. F., Aydın, S., & Koşar, P. N. (2016). Radyasyon Güvenliğinde Mesleki Olarak Bilmemiz Gerekenler. SDÜ SAĞLIK BİLİMLERİ DERGİSİ, 7(2), 35–35. https://doi.org/10.22312/sdusbed.261237

[27] Dönmez, S. (2017). Radiation detection and measurement. Nuclear Medicine Seminars, 3(3), 172–177. https://doi.org/10.4274/nts.2017.018

[28] Cecen, G. S. (2015). Radiation in the Orthopaedic Operating Theatre. ACTA ORTHOPAEDICA et TRAUMATOLOGICA TURCICA. https://doi.org/10.3944/aott.2015.14.0250

[29] Günay, O., Gündoğdu, Ö., Demir, M., İper, H. S. T., İhsan, K. U. R. U., Yaşar, D., ... & YARAR, O. (2020). Determination of absorbed radiation dose levels of lenses thyroid and oral mucosa in computed tomography imagining: Phantom Study. Kocaeli Üniversitesi Sağlık Bilimleri Dergisi, 6(1), 23–27. https://doi.org/10.30934/kusbed.603335